

# Use of vector polarizability to manipulate alkali-metal atoms

D. Cho\*

*Department of Physics, Korea University, Seoul 02841, Korea*

(Dated: March 23, 2023)

## Abstract

We review a few ideas and experiments that our laboratory at Korea University has proposed and carried out to use vector polarizability  $\beta$  to manipulate alkali-metal atoms.  $\beta$  comes from spin-orbit coupling, and it produces an ac Stark shift that resembles a Zeeman shift. When a circularly polarized laser field is properly detuned between the  $D_1$  and  $D_2$  transitions, an ac Stark shift of a ground-state atom takes the form of a pure Zeeman shift. We call it the “analogous Zeeman effect”, and experimentally demonstrated an optical Stern-Gerlach effect and an optical trap that behaves exactly like a magnetic trap. By tuning polarization of a trapping beam, and thereby controlling a shift proportional to  $\beta$ , we demonstrated elimination of an inhomogeneous broadening of a ground hyperfine transition in an optical trap. We call it “magic polarization”. We also showed significant narrowing of a Raman sideband transition at a specific well depth. A Raman sideband in an optical trap is broadened owing to anharmonicity of the trap potential, and the broadening can be eliminated by a  $\beta$ -induced differential ac Stark shift at what we call a “magic well depth”. Finally, we proposed and experimentally demonstrated a cooling scheme that incorporated the idea of velocity-selective coherent population trapping to Raman sideband cooling to enhance cooling efficiency of the latter outside of the Lamb-Dicke regime. We call it “motion-selective coherent population trapping”, and  $\beta$  is responsible for the selectivity. We include as Supplementary Material a program file that calculates both scalar and vector polarizabilities of a given alkali-metal atom when the wavelength of an applied field is specified. It also calculates depth of a potential well and photon-scattering rate of a trapped atom in a specific ground state when power, minimum spot size, and polarization of a trap beam are given.

---

\* e-mail address: cho@korea.ac.kr

## I. INTRODUCTION

While a near-resonant laser field applies radiation pressure on an atom, an off-resonant one can produce an energy shift by the ac Stark effect. The former plays an important role in slowing and cooling atoms at an ambient temperature, and the latter, coupled with an intensity gradient, produces an electric dipole force to trap precooled atoms. When the laser field is far detuned from allowed transitions, an optical dipole trap provides an almost conservative potential well, which is ideal for precision spectroscopy or quantum manipulation of trapped atoms. In addition, the ac Stark shift of an alkali-metal atom in an elliptically polarized laser field depends on the magnetic quantum number of the atom and degree of circularity of the field. This dependence gives us a versatile tool to manipulate an alkali-metal atom in an optical trap. In this paper, I will review a few ideas and experiments that our group at Korea University has proposed and performed to use this useful tool.

We first introduce spherical tensor formalism of the ac Stark shift to quantify its polarization dependence in terms of a vector polarizability. The theory section is followed by one on the analogous Zeeman effect [1, 2], where we show that when an applied field is circularly polarized and detuned properly between the  $D_1$  and  $D_2$  transitions, an ac Stark shift takes the form of a pure Zeeman shift. The intensity gradient of such a field produces optical Stern-Gerlach effect [3] or an optical trap that behaves like a magnetic trap [4]. Next two sections describe “magic” ideas; (i) A shift proportional to vector polarizability can be used to eliminate an inhomogeneous broadening of a ground hyperfine transition, which originates from the difference in scalar polarizabilities of the two hyperfine levels. The elimination is complete at a particular polarization, and we call it magic polarization [5, 6]. (ii) Stimulated Raman transitions of a trapped atom that involve the change in vibrational quantum number show inhomogeneous broadening from anharmonicity of an optical trap. It can be eliminated by another broadening from the vector polarizability. Anharmonicity-induced broadening is independent of well depth, and we use the well depth as a tuning parameter to eliminate the broadening. We call it magic well depth [7]. Finally, we describe a cooling method that we call motion-selective coherent population trapping [8, 9]. In this method, the ideas of Raman sideband cooling and velocity-selective coherent population trapping are combined to complement each other, and vector polarizability plays a pivotal role in producing motion-selectivity.

## II. SPHERICAL TENSOR FORMALISM OF AC STARK SHIFT

When an atom in the state  $|\Psi_0\rangle$  is irradiated by a laser field with an oscillating electric field  $\vec{E}(t) = \vec{\mathcal{E}}e^{-i\omega t} + \vec{\mathcal{E}}^*e^{i\omega t}$ , its ac Stark shift is, from second-order perturbation theory,

$$U_{\text{AC}}(\Psi_0) = \sum_{n \neq 0} \frac{\langle \Psi_0 | \vec{d} \cdot \vec{\mathcal{E}}^* | \Psi_n \rangle \langle \Psi_n | \vec{d} \cdot \vec{\mathcal{E}} | \Psi_0 \rangle}{\hbar[\omega - (\omega_n - \omega_0)]} - \sum_{n \neq 0} \frac{\langle \Psi_0 | \vec{d} \cdot \vec{\mathcal{E}} | \Psi_n \rangle \langle \Psi_n | \vec{d} \cdot \vec{\mathcal{E}}^* | \Psi_0 \rangle}{\hbar[\omega + (\omega_n - \omega_0)]}, \quad (1)$$

where  $\omega_0$  and  $\omega_n$  are the unperturbed energy eigenvalues of  $|\Psi_0\rangle$  and  $|\Psi_n\rangle$ , respectively, and  $\vec{d}$  is the electric dipole moment operator. When  $|\Psi_0\rangle$  is the ground state, the second term is off resonant and it is much smaller than the first in most cases.  $U_{\text{AC}}(\Psi_0)$  can be written as  $\langle \Psi_0 | \Omega_+ + \Omega_- | \Psi_0 \rangle$ , where

$$\Omega_+ = \sum_{i,j} d_i \mathcal{E}_i^* (\omega - H + \omega_0)^{-1} d_j \mathcal{E}_j, \quad (2)$$

$$\Omega_- = \sum_{i,j} d_i \mathcal{E}_i (-\omega - H + \omega_0)^{-1} d_j \mathcal{E}_j^*, \quad (3)$$

where  $H$  is the unperturbed atomic Hamiltonian, and  $\mathcal{E}_i$ ,  $\mathcal{E}_j$  and  $d_i$ ,  $d_j$  for  $i, j = x, y, z$  are the Cartesian components of  $\vec{\mathcal{E}}$  and  $\vec{d}$ , respectively. The operators can be rewritten in a spherical tensor form [10], and explicitly for  $\Omega_+$ ,

$$\Omega_+ = \sum_{L=0}^2 (-1)^L \sum_{m=-L}^L (-1)^m \mathcal{D}_m^{(L)} \mathcal{F}_{-m}^{(L)}, \quad (4)$$

where  $\mathcal{D}^{(L)}$  and  $\mathcal{F}^{(L)}$  with  $L = 0, 1, 2$  are the scalar, vector and the second-rank spherical tensor operators:

$$\mathcal{D}_m^{(L)} = (-1)^{m+1} \sqrt{2L+1} \sum_{\mu=-1}^1 \begin{pmatrix} 1 & 1 & L \\ \mu & m-\mu & -m \end{pmatrix} d_\mu (\omega_0 - H_0 + \omega)^{-1} d_{m-\mu}. \quad (5)$$

Here  $d_0 = z$  and  $d_{\pm 1} = \mp(x \pm iy)/\sqrt{2}$ .  $\mathcal{F}_m^{(L)}$  are similarly defined in terms of  $\mathcal{E}_i^*$  and  $\mathcal{E}_j$ ;

$$\mathcal{F}_m^{(L)} = (-1)^{m+1} \sqrt{2L+1} \sum_{\mu=-1}^1 \begin{pmatrix} 1 & 1 & L \\ \mu & m-\mu & -m \end{pmatrix} \mathcal{E}_\mu^* \mathcal{E}_{m-\mu}, \quad (6)$$

where  $\mathcal{E}_0 = \mathcal{E}_z$  and  $\mathcal{E}_{\pm 1} = \mp(\mathcal{E}_x \pm i\mathcal{E}_y)/\sqrt{2}$ .  $\Omega_-$  can be similarly reformulated.

While the scalar term in  $U_{\text{AC}}(\Psi_0)$  is simply proportional to  $|\vec{\mathcal{E}}|^2$ , the vector term is proportional to  $\langle \Psi_0 | \vec{\sigma} | \Psi_0 \rangle \cdot (\vec{\mathcal{E}} \times \vec{\mathcal{E}}^*)$  leading to dependence of the ac Stark shift on magnetic quantum number of the atom and polarization of the field. Here,  $\mathcal{D}^{(1)}$  in the vector term

is replaced with the Pauli spin operator using the Wigner-Eckart theorem. The second-rank term is nonvanishing only if the total angular momentum of the state  $\Psi_0$  is at least 1. Although the ground state of an alkali-metal atom has a nuclear spin in addition to the electron spin 1/2 so that the total angular momentum  $F$  can be larger than 1, when the detuning of the field  $\vec{E}(t)$  from the  $D$  transitions is much larger than the hyperfine splitting, the second-rank term can be neglected. Under this approximation, the ac Stark shift of the ground hyperfine state  $|nS_{1/2}, F, m_F\rangle$  of an alkali-metal atom, where  $m_F$  is the magnetic quantum number, can be written as

$$U_{AC}(F, m_F) = \alpha |\vec{\mathcal{E}}|^2 - i\beta \langle S_{1/2}, F, m_F | \vec{\sigma} | S_{1/2}, F, m_F \rangle \cdot (\vec{\mathcal{E}} \times \vec{\mathcal{E}}^*), \quad (7)$$

where  $\alpha$  and  $\beta$  are the scalar and the vector polarizabilities, respectively. Their expressions can be obtained by comparing Eq. (1) with Eq. (7):

$$\alpha = \frac{1}{6\hbar} \sum_{n'} |\langle n' P_{1/2} || d || n S_{1/2} \rangle|^2 \left[ \frac{1}{\omega - (\omega_{n' P_{1/2}} - \omega_{n S_{1/2}})} - \frac{1}{\omega + (\omega_{n' P_{1/2}} - \omega_{n S_{1/2}})} \right] \quad (8)$$

$$+ \frac{1}{6\hbar} \sum_{n'} |\langle n' P_{3/2} || d || n S_{1/2} \rangle|^2 \left[ \frac{1}{\omega - (\omega_{n' P_{3/2}} - \omega_{n S_{1/2}})} - \frac{1}{\omega + (\omega_{n' P_{3/2}} - \omega_{n S_{1/2}})} \right],$$

$$\beta = \frac{1}{6\hbar} \sum_{n'} |\langle n' P_{1/2} || d || n S_{1/2} \rangle|^2 \left[ \frac{1}{\omega - (\omega_{n' P_{1/2}} - \omega_{n S_{1/2}})} + \frac{1}{\omega + (\omega_{n' P_{1/2}} - \omega_{n S_{1/2}})} \right] \quad (9)$$

$$- \frac{1}{12\hbar} \sum_{n'} |\langle n' P_{3/2} || d || n S_{1/2} \rangle|^2 \left[ \frac{1}{\omega - (\omega_{n' P_{3/2}} - \omega_{n S_{1/2}})} + \frac{1}{\omega + (\omega_{n' P_{3/2}} - \omega_{n S_{1/2}})} \right],$$

where  $\langle n' P_J || d || n S_{1/2} \rangle$  for  $J = 1/2$  and  $3/2$  is the reduced matrix element of  $\vec{d}$ . The definition of  $\langle n' P_J || d || n S_{1/2} \rangle$  we use is given in Appendix A.

The ac Stark shift in Eq. (7) can be written in a form which clearly shows its dependence on  $m_F$  and polarization of the laser beam:

$$U_{AC}(F, m_F) = (\alpha - \eta \beta g_F m_F) (c \mu_0 I_0 / 2), \quad (10)$$

where  $I_0 = 2|\vec{\mathcal{E}}|^2 / c \mu_0$  is the intensity of the laser field  $\vec{E}(t) = \vec{\mathcal{E}} e^{-i\omega t} + \vec{\mathcal{E}}^* e^{i\omega t}$ ,  $g_F$  is the Landé  $g$  factor, and  $\eta$  is the degree of circularity:

$$\eta = i \hat{z} \cdot (\hat{\epsilon} \times \hat{\epsilon}^*). \quad (11)$$

Here  $\hat{\epsilon}$  is a Jones vector for the field  $\vec{\mathcal{E}}$  and  $\hat{z}$  is the quantization axis that defines  $m_F$ .  $\eta$  is 0 for a linearly polarized light, and +1 and -1 for a right and a left circularly polarized

light, respectively, when the light propagates along  $\hat{z}$ . We note that the second term has the same form as a Zeeman shift,  $g_F m_F \mu_B B_0$ , of an atom in the  $|nS_{1/2}, F, m_F\rangle$  state inside a magnetic field  $B_0 \hat{z}$ , and we define an effective magnetic field,

$$\mathcal{B}_{\text{eff}} = -\frac{\eta\beta c\mu_0 I_0}{2\mu_B}, \quad (12)$$

where  $\mu_B$  is the Bohr magneton. To understand the origin of this Zeeman-like ac Stark shift, we write  $U_{\text{AC}}(F, m_F)$  in Eq. (7) as an expectation value of an electric dipole interaction Hamiltonian,  $-\vec{d}_{\text{ind}}(\vec{\mathcal{E}}) \cdot \vec{\mathcal{E}}^*$ , where

$$\vec{d}_{\text{ind}}(\vec{\mathcal{E}}) = -\alpha\vec{\mathcal{E}} + i\beta(\vec{\sigma} \times \vec{\mathcal{E}}) \quad (13)$$

is an induced electric dipole moment. While the scalar term is from the usual polarization by  $\vec{\mathcal{E}}$  and parallel to the field, the vector term is from perturbation by the spin-orbit coupling and is perpendicular to the field. The spin-orbit coupling mediates the interaction between the magnetic dipole moment of an electron with  $\vec{E}(t)$ , while their direct interaction is forbidden by parity ( $P$ ) and the time-reversal ( $T$ ) symmetry. We point out that the second term in Eq. (13) is odd under  $P$  and even under  $T$  like an electric dipole moment, and the equation satisfies  $P$  and  $T$  symmetry. According to this picture,  $\beta$  depends on the strength of the spin-orbit coupling. This can be shown by rewriting  $\alpha$  and  $\beta$  in Eqs. (8, 9) as

$$\alpha \approx \frac{1}{6\hbar} \sum_{n'} |\langle n' P_{1/2} || d || n S_{1/2} \rangle|^2 \left[ \frac{1}{\Delta_1(n')} + \frac{2}{\Delta_2(n')} \right], \quad (14)$$

$$\beta \approx \frac{1}{6\hbar} \sum_{n'} |\langle n' P_{1/2} || d || n S_{1/2} \rangle|^2 \left[ \frac{1}{\Delta_1(n')} - \frac{1}{\Delta_2(n')} \right], \quad (15)$$

where  $\Delta_1(n') = \omega - (\omega_{n' P_{1/2}} - \omega_{n S_{1/2}})$  and  $\Delta_2(n') = \omega - (\omega_{n' P_{3/2}} - \omega_{n S_{1/2}})$ . Here we use  $|\langle n' P_{3/2} || d || n S_{1/2} \rangle|^2 \approx 2|\langle n' P_{1/2} || d || n S_{1/2} \rangle|^2$  and neglect the off-resonant terms. Without the spin-orbit coupling, there is no fine structure and  $\Delta_1(n') = \Delta_2(n')$  and  $\beta = 0$ . As a consequence, heavy alkali-metal atoms with a strong spin-orbit coupling such as Rb and Cs have larger  $\beta$  than the lighter atoms.

In an optical trap, in addition to the ac Stark shift  $U_{\text{AC}}$  in Eq. (1), which determines well depth, the rate of scattering  $R_\gamma$  of the trap beam by an atom, which determines heating and decoherence rate, is also an important parameter. Using first-order time-dependent perturbation theory, the scattering rate is given by

$$R_\gamma(\Psi_0) \approx \sum_{n \neq 0} \frac{\langle \Psi_0 | \vec{d} \cdot \vec{\mathcal{E}}^* | \Psi_n \rangle \langle \Psi_n | \vec{d} \cdot \vec{\mathcal{E}} | \Psi_0 \rangle}{\hbar^2 \{ \omega - (\omega_n - \omega_0) \}^2} \Gamma(n), \quad (16)$$

where  $\Gamma(n) = 1/\tau(n)$  with  $\tau(n)$  being a lifetime of the upper state  $|\Psi_n\rangle$ , and the off-resonant terms are neglected. If we further assume that  $\Gamma(n)$  is independent of  $n$ ,  $R_\gamma(\Psi_0)$  can be written as  $\langle\Psi_0|\Theta|\Psi_0\rangle\Gamma$ , where

$$\Theta = \sum_{i,j} d_i \mathcal{E}_i^* (\omega - H + \omega_0)^{-2} d_j \mathcal{E}_j, \quad (17)$$

which is similar to  $\Omega_\pm$  in Eqs. (2, 3). When  $|\Psi_0\rangle$  is the ground state of an alkali-metal atom and a trap beam is red detuned from the  $D$  transitions, only the contributions from the  $D_1$  and  $D_2$  transitions to  $R_\gamma(\Psi_0)$  are significant and we may neglect couplings to the higher excited states. In addition, decay rates of the  $nP_{1/2}$  and  $nP_{3/2}$  states are approximately the same. Under these approximations, the transformation of  $R_\gamma(\Psi_0)$  in Eq. (16) to  $\langle\Psi_0|\Theta|\Psi_0\rangle\Gamma$  is justified. Following the spherical tensor formalism that led to Eq. (10), the photon scattering rate of the ground hyperfine state  $|nS_{1/2}, F, m_F\rangle$  of an alkali-metal atom can be approximated as

$$R_\gamma(F, m_F) = (a - \eta b g_F m_F) (c\mu_0 I_0 / 2) \Gamma, \quad (18)$$

where considering only the  $D_1$  and  $D_2$  couplings,

$$a = \frac{1}{6\hbar^2} \left[ \frac{|\langle nP_{1/2} || d || nS_{1/2} \rangle|^2}{\{\omega - (\omega_{nP_{1/2}} - \omega_{nS_{1/2}})\}^2} + \frac{|\langle nP_{3/2} || d || nS_{1/2} \rangle|^2}{\{\omega - (\omega_{nP_{3/2}} - \omega_{nS_{1/2}})\}^2} \right], \quad (19)$$

$$b = \frac{1}{12\hbar^2} \left[ \frac{2|\langle nP_{1/2} || d || nS_{1/2} \rangle|^2}{\{\omega - (\omega_{nP_{1/2}} - \omega_{nS_{1/2}})\}^2} - \frac{|\langle nP_{3/2} || d || nS_{1/2} \rangle|^2}{\{\omega - (\omega_{nP_{3/2}} - \omega_{nS_{1/2}})\}^2} \right]. \quad (20)$$

In the Supplementary Material, we include a Microsoft Excel file that calculates  $\alpha, \beta$  and  $a, b$  of alkali-metal atoms from lithium to cesium when the wavelength of an applied laser beam is given. Because we consider a far-detuned trap beam, effects of nuclear spin and isotope shift on the polarizabilities and the scattering parameters are negligible. For a given ground hyperfine state  $|nS_{1/2}, F, m_F\rangle$ , the Excel file calculates well depth  $U_{AC}(F, m_F)$  and photon scattering rate  $R_\gamma(F, m_F)$  of an optical trap according to Eq. (10) and Eq. (18), respectively, when power, minimum spot size, and degree of circularity  $\eta$  of the trap beam are given. Formulae and conversion factors used for the items in the Excel file are explained in Appendix A.

### III. ANALOGOUS ZEEMAN EFFECT

In a typical optical trap, a trap beam is far red detuned from the  $D_1$  transition as shown in Fig. 1(a). Here, we consider a case of tuning the beam between the  $D_1$  and  $D_2$  transitions as in Fig. 1(b). In this case,  $\Delta_1(n)$  and  $\Delta_2(n)$  have opposite signs, and we note from Eqs. (14, 15) that  $\alpha$  tends to be suppressed while  $\beta$  tends to be enhanced. Especially when

$$\Delta_2(n) = -2\Delta_1(n), \quad (21)$$

neglecting couplings other than  $D_1$  and  $D_2$ ,  $\alpha$  vanishes and the ac Stark shift becomes

$$U_{AC}(F, m_F) = -\eta\beta g_F m_F (c\mu_0 I_0/2). \quad (22)$$

It is identical to a Zeeman shift of the  $|nS_{1/2}, F, m_F\rangle$  state of an alkali-metal atom with an effective magnetic field  $\mathcal{B}_{\text{eff}}$  given in Eq. (12). We call it the analogous Zeeman effect [1], which makes a laser beam play the role of a magnetic field with the field strength proportional to its intensity. This effect gives a versatile tool to manipulate alkali-metal atoms. However, it is applicable to only heavy alkali-metal atoms such as Rb and Cs with large fine structure. For the lighter atoms, the small fine structure limits detuning. Because  $R_\gamma$  in Eq. (16) is inversely proportional to the detuning squared, excessive scattering of the trap beam becomes a problem. In Table I, for each alkali-metal atom, the wavelength  $\lambda_0$  that satisfies the condition of Eq. (21) and  $\beta$  at  $\lambda_0$  are given.  $\mathcal{B}_{\text{eff}}$  and  $R_\gamma$  for a state with  $g_F m_F = 1$  are also tabulated when the laser intensity  $I_0$  is  $1.4 \times 10^9 \text{ W/m}^2$ , corresponding to laser power of 0.5 W and minimum spot size of  $15 \text{ }\mu\text{m}$ , and with right-circular polarization so that  $\eta = 1$ .

We experimentally confirmed the Zeeman-like ac Stark shift of Eq. (22) by performing stimulated Raman spectroscopy [2] on a slow Rb beam leaked from a magneto-optical trap [14]. The intensity gradient of an elliptically polarized beam with a detuning of Eq. (21) exerts an  $m_F$ -dependent force on an alkali-metal atom in the same way as a magnetic field gradient does. The strength of the force is proportional to the degree of circularity  $\eta$  in Eq. (11). We demonstrated that a spin-polarized Rb atom traversing an intensity gradient on one side of a Gaussian beam profile showed  $\eta$ -dependent deflection [3]. The experimental apparatus is shown in Fig. 2, and the results are shown in Fig. 3; for the right and left circularly polarized beam of  $\eta = +1$  and  $-1$ , respectively, atoms are deflected in the opposite

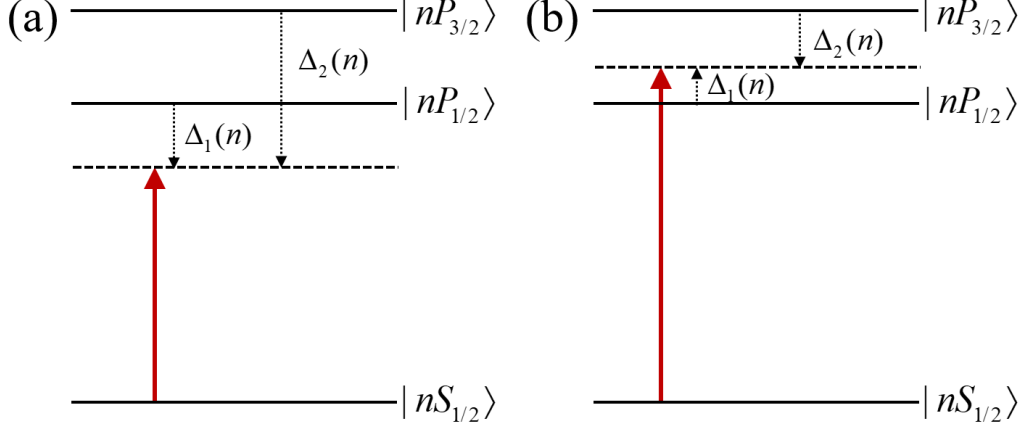


FIG. 1: (a) A trap beam can be either red detuned from the  $D_1$  transition or (b) tuned between the  $D_1$  and  $D_2$  transitions.

TABLE I: Parameters for analogous Zeeman effect.  $\lambda_0$  is the wavelength that satisfies Eq. (21),  $\beta$  is the vector polarizability at  $\lambda_0$ .  $\mathcal{B}_{\text{eff}}$  and  $R_\gamma$  are effective magnetic field and photon scattering rate, respectively, for a state with  $g_F m_F = 1$  when the laser intensity is  $1.4 \times 10^9$  W/m<sup>2</sup> with right-circular polarization.

atom	$\lambda_0$ (nm)	$\beta$ (atomic units)	$\mathcal{B}_{\text{eff}}$ (G)	$R_\gamma$ (s <sup>-1</sup> )
Li	670.8	$5.4 \times 10^6$	$2.5 \times 10^4$	$2.0 \times 10^8$
Na	589.4	$1.2 \times 10^5$	560	$1.4 \times 10^5$
K	768.8	$4.8 \times 10^4$	230	$1.0 \times 10^4$
Rb	789.8	$1.2 \times 10^4$	58	$6.5 \times 10^2$
Cs	879.8	$6.0 \times 10^3$	28	$1.2 \times 10^2$

directions. We call it optical the Stern-Gerlach effect. While the term was used to describe the difference in radiation pressure experienced by two states of a fictitious spin associated with a two-level atom [15, 16], our experiment is a more direct analogy to the original Stern-Gerlach experiment. We also used the idea to create an optical trap that behaves like a magnetic trap and observed 98% spin polarization of the trapped atoms [4]. This idea has been applied to many interesting experiments. As an example, in a quantum walk experiment in a one dimensional optical lattice, the optical Stern-Gerlach force by a circularly polarized lattice beam plays the role of a coin toss on an atom in a superposition of opposite  $g_F m_F$  states [17]. Quantum gate operation by entangling two atoms in a three dimensional



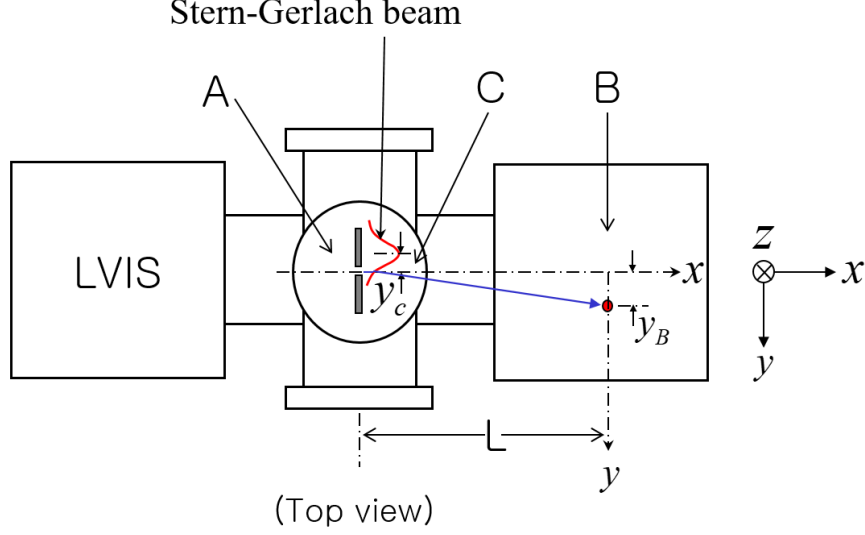


FIG. 2: Apparatus for the optical Stern-Gerlach experiment. It consists of a low-velocity intense source of atoms, a spin-polarization region (A), an interaction region (C), and a probe region (B). In the C region, a vertically propagating Gaussian beam is tightly focused.

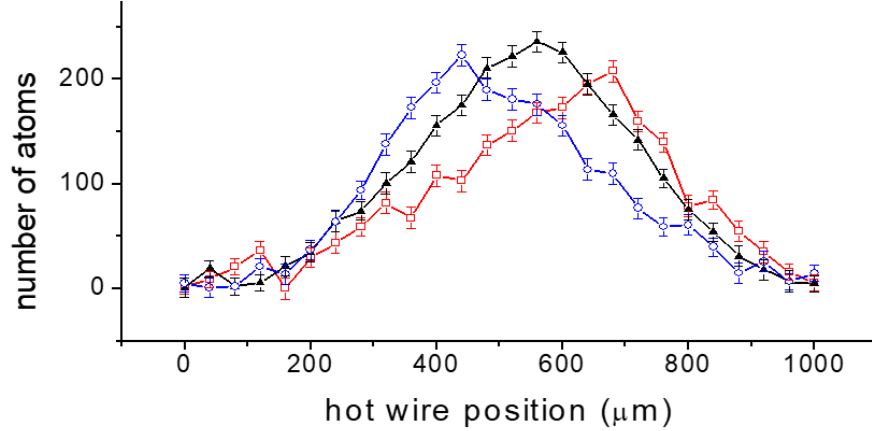


FIG. 3: Hot-wire scan results. Triangles are when the Stern-Gerlach beam is blocked. Circles and squares are when the Stern-Gerlach beam is right and left circularly polarized, respectively.

optical lattice was realized by merging nearby sites by controlling lattice polarization [18].

#### IV. MAGIC POLARIZATION

Motivation of the early research on laser cooling and trapping of atoms in the 1980s was to increase interrogation time to improve precision in spectroscopy. However, an optically trapped atom suffers a state-dependent ac Stark shift, which leads to inhomogeneous broadening of a transition, and most of the benefit of long interrogation time is lost. For an

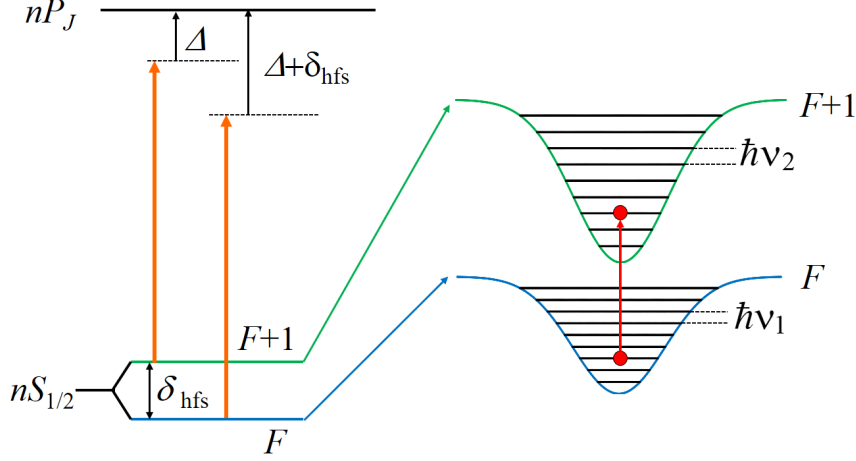


FIG. 4: Inhomogeneous broadening of a ground hyperfine transition of an alkali-metal atom.

optical transition, such as the  $D$  transitions of an alkali-metal atom, the idea of magic wavelength can eliminate the broadening when there is a proper three-level configuration [19]. For a ground hyperfine transition of an alkali-metal atom, the inhomogeneous broadening originates from different detuning for the  $F$  and  $F + 1$  states owing to the ground hyperfine splitting  $\delta_{\text{hfs}}$  as shown in Fig. 4. Atoms in the  $F$  and  $F + 1$  states have different ac Stark shifts, and consequently their well depths  $U_1$  and  $U_2$  and vibration frequencies  $\nu_1$  and  $\nu_2$ , respectively, are different. This implies that transition frequency between the vibrational states  $|\chi_1(n)\rangle$  and  $|\chi_2(n)\rangle$  of  $U_1$  and  $U_2$ , respectively, depends on the vibrational quantum number  $n$ , and even a transition between  $|\chi_1(n_1)\rangle$  and  $|\chi_2(n_2)\rangle$  with  $n_1 \neq n_2$  is possible.

Because the ground hyperfine transition plays an important role in precision measurement such as an atomic clock and search for symmetry violation, there were many discussions [20] and experimental efforts to overcome this problem: for example, use of an extra laser beam to compensate the differential shift [21, 22], spin-echo or dynamic decoupling to undo Stark-induced dephasing [23], and a blue-detuned optical bottle to minimize atom-light interaction [24]. However, these approaches are designed only to reduce the broadening and dephasing. In 2007, we proposed an idea that could eliminate the differential shift completely by having  $U_1 = U_2$  for a transition of interest [5]. The idea relies on the  $\beta$ -induced ac Stark shift in Eq. (10) again; for a transition from the  $|nS_{1/2}, F, m_F\rangle$  to the  $|nS_{1/2}, F + 1, m'_F\rangle$  state, the differential shift vanishes when the degree of circularity satisfies

$$\eta = \frac{\Delta\alpha}{\beta g_F(m_F + m'_F)}, \quad (23)$$

where  $\Delta\alpha = \alpha_{F+1} - \alpha_F$  with  $\alpha_{F+1}$  and  $\alpha_F$  being the scalar polarizabilities of the  $F + 1$  and  $F$  state, respectively, and  $\beta$  is an average value of those for the  $F + 1$  and  $F$  states. We call it the magic polarization. The same idea was published in 2008 by a theory group [25], who proposed to tune the angle  $\theta$  between a quantization axis defined by a magnetic field and trap-beam propagation direction to eliminate the differential ac Stark shift by noting that the effective degree of circularity is given by

$$\eta_{\text{eff}} = \eta \cos \theta. \quad (24)$$

Although both proposals in Refs. [5] and [25] considered a hyperfine transition of an optically trapped Cs atom, it is not the best atom to apply the idea because its large  $\beta$  puts very stringent limit on polarization control. Optically trapped atoms at temperature  $T$  have an average vibrational quantum number  $\langle n \rangle = k_B T / \hbar \nu$  in a one-dimensional model, where  $k_B$  is the Boltzmann constant. When a polarization error results in  $\delta\eta$  from the magic condition in Eq. (23), frequency of a  $\Delta n = 0$  transition for  $n = \langle n \rangle$  is shifted by  $\delta f$  from that for  $n = 0$  with  $\delta\eta$  and  $\delta f$  being related by

$$\delta\eta = \frac{\alpha}{\beta g_F(m_F + m'_F)} \cdot \frac{h}{k_B T} \delta f. \quad (25)$$

Any imperfection in polarization-control optics such as a linear polarizer or a retardation plate and residual birefringence of a lens or a window can introduce  $\delta\eta$ . We note that for

TABLE II: Tolerance on polarization control for most abundant isotopes of alkali-metal atoms.  $\lambda_{\text{trap}}$  is the wavelength when a trap beam is 100 THz red detuned from the  $D_1$  transition.  $f_{\text{hf}}$  is the ground hyperfine splitting.  $\alpha$  and  $\beta$  at  $\lambda_{\text{trap}}$  are given in atomic units.  $\eta_{\text{magic}}$  satisfies the magic-polarization condition in Eq. (23) when  $g_F(m_F + m'_F) = 1$ , and  $\delta\eta_{\text{max}}$  is tolerance on  $\eta$  when  $\delta f = 1$  Hz and atomic temperature is 100  $\mu\text{K}$ .

atom	$\lambda_{\text{trap}}$ (nm)	$f_{\text{hf}}$ (GHz)	$\alpha$ (a.u.)	$\beta$ (a.u.)	$\eta_{\text{magic}}$	$\delta\eta_{\text{max}}$
$^7\text{Li}$	864	0.803	407	0.016	0.18	$1.2 \times 10^{-2}$
$^{23}\text{Na}$	734	1.772	453	0.66	$1.1 \times 10^{-2}$	$3.3 \times 10^{-4}$
$^{39}\text{K}$	1036	0.462	629	3.3	$7.5 \times 10^{-4}$	$9.2 \times 10^{-5}$
$^{87}\text{Rb}$	1082	6.835	652	13	$2.8 \times 10^{-3}$	$2.4 \times 10^{-5}$
$^{133}\text{Cs}$	1275	9.193	714	32	$1.5 \times 10^{-3}$	$1.1 \times 10^{-5}$

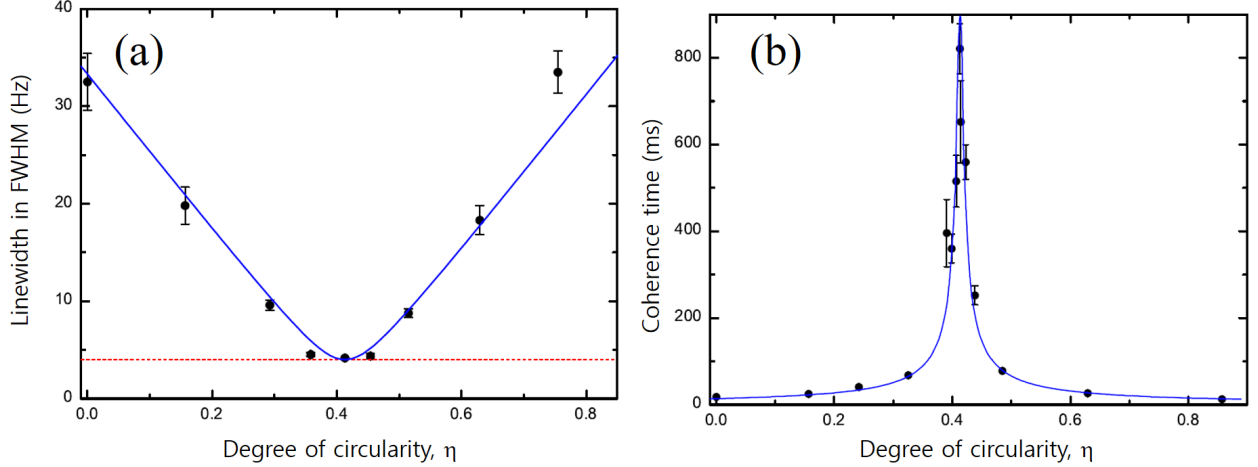


FIG. 5: (a) Full width at half maximum when rf field is applied for 200 ms and (b) coherence time of the  $|2S_{1/2}, F = 1, m_F = 1\rangle$  to  $|2S_{1/2}, F = 2, m_F = 2\rangle$  transition of  $^7\text{Li}$  atoms in a 1064-nm optical trap versus degree of circularity  $\eta$ .

a given  $\delta f$ , tolerance  $\delta\eta_{\text{max}}$  on polarization control is inversely proportional to  $\beta$ , and it becomes small for heavy atoms. In Table II,  $\delta\eta_{\text{max}}$  for  $\delta f = 1$  Hz is given when a trap beam is 100 THz red detuned from the  $D_1$  transition,  $T = 100$   $\mu\text{K}$ , and  $g_F(m_F + m'_F) = 1$ . For experimental demonstration of magic polarization, we used the  $|2S_{1/2}, F = 1, m_F = 1\rangle$  to  $|2S_{1/2}, F = 2, m_F = 2\rangle$  transition of  $^7\text{Li}$  atoms in a 1064-nm optical trap [6]. Fig. 5(a) and (b) show full width at half maximum (FWHM) of Rabi lineshape and coherence time  $\tau_c$  from Ramsey spectroscopy, respectively, versus  $\eta$ . We observed minimum linewidth and maximum  $\tau_c$  at  $\eta = 0.413$  while  $\eta_{\text{magic}}$  calculated from the published data [26] is 0.39. When we applied 803-MHz field for 2 s, FWHM was as small as  $0.59 \pm 0.02$  Hz, while the Fourier-limited value was 0.4 Hz. The maximum  $\tau_c$  in Fig. 5(b) was  $820 \pm 60$  ms, largely limited by magnetic field noise.

The narrow linewidth allowed us to address individual Li atoms in a 1D optical lattice with a site-specific resolution, and the long coherence time allowed us to coherently manipulate individual atoms independently of neighboring ones [27]. Figure 6 shows Rabi signal from single atoms at three adjacent sites versus rf frequency while a magnetic field gradient along the lattice introduces differential Zeeman shift  $\Delta f_{\text{Zeeman}}$  of 180 Hz between neighboring sites. Resolving power in the frequency domain, defined as  $\Delta f_{\text{Zeeman}}$  divided by FWHM of each Rabi lineshape, is 2.3. It is three times that in the spatial domain of 0.8 obtained by a state-of-the-art quantum-gas microscope on Li atoms in an optical lattice [28]. Here, the

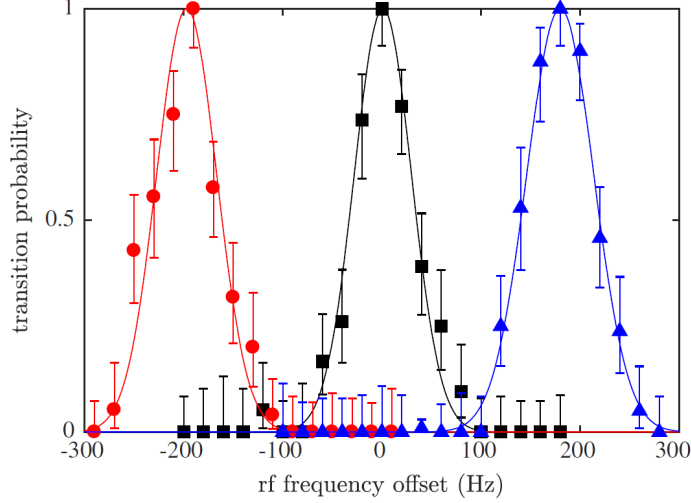


FIG. 6: Rabi line shapes for single atoms residing at the  $q_{-1}$  (red circle),  $q_0$  (black square), and  $q_{+1}$  sites (blue triangle). Magnetic field gradient is 1.6 G/cm. Solid curves are theory predictions for a  $\pi$  pulse driven by a 20-ms Blackman window.

resolving power in the spatial domain is defined as half the lattice wavelength divided by FWHM of a point spread function of an imaging optics.

For a clock transition between  $m_F = 0$  states, where the first-order Zeeman shift vanishes and the idea of magic polarization is not applicable, Derevianko proposed to use the second-order shift to eliminate the inhomogeneous broadening [29]. When  $\vec{B} = B_0 \hat{z}$  is applied, the second-order Zeeman shift of a clock transition at  $f_0$  is

$$\Delta f_Z^{(2)} \approx 2f_0 \left( \frac{\mu_B B_0}{h f_0} \right)^2. \quad (26)$$

In addition, inside a right circularly polarized trap beam, the total shift  $\Delta f_0$  of the clock transition is given by

$$h\Delta f_0 = \Delta\alpha |\vec{\mathcal{E}}|^2 + \frac{2\mu_B^2}{h f_0} \left( B_0 - \frac{\beta}{\mu_B} |\vec{\mathcal{E}}|^2 \right)^2, \quad (27)$$

where  $\Delta\alpha = \alpha_{F+1} - \alpha_F$  and  $B_0$  in Eq. (26) is replaced by  $B_0 + \mathcal{B}_{\text{eff}}$ . Inhomogeneous broadening owing to  $\Delta\alpha$  is eliminated when

$$B_0 = \frac{\Delta\alpha}{\beta} \cdot \frac{h f_0}{4\mu_B}, \quad (28)$$

which may be called a magic B field. Effect from  $|\mathcal{B}_{\text{eff}}|^2$  is negligible for an alkali-metal atom owing to the smallness of  $|\mu_B \mathcal{B}_{\text{eff}} / h f_0|$  in a typical optical trap.

## V. MAGIC WELL DEPTH

One of the most effective ways to cool trapped atoms is Raman sideband cooling (RSC) [30]. We consider RSC applied to alkali-metal atoms trapped in a 1D optical lattice formed by a standing wave of a Gaussian beam with a minimum spot size  $w_0$  and wavelength  $\lambda_{\text{OL}}$ . Its potential well is

$$U(\vec{r}) = U_0 e^{-2(x^2+y^2)/w_0^2} \cos^2 kz, \quad (29)$$

where  $U_0 = U_{\text{AC}}(F, m_F)$  in Eq. (10) and  $k = 2\pi/\lambda_{\text{OL}}$ . We assume a large Rayleigh range and therefore a constant spot size. In a harmonic approximation, the state of a lattice-bound atom is described by  $|\psi_j(\mathbf{n})\rangle = |\phi_j\rangle \otimes |\chi(\mathbf{n})\rangle$ , where  $|\phi_j\rangle$  is one of the ground hyperfine states and  $|\chi(\mathbf{n})\rangle$  with vibrational quantum numbers  $\mathbf{n} = (n_x, n_y, n_z)$  represents a 3D harmonic oscillator. Longitudinal and transverse vibration frequencies are  $\nu_z = k\sqrt{2|U_0|/m}$  and  $\nu_\perp = (2/w_0)\sqrt{|U_0|/m}$ , respectively, with  $m$  being the atomic mass. For RSC along the  $z$  axis, we use a Raman transition  $|\psi_1(\mathbf{n})\rangle \rightarrow |\psi_2(\mathbf{n}')\rangle$  with  $|\phi_1\rangle = |nS_{1/2}, F, m_F\rangle$ ,  $|\phi_2\rangle = |nS_{1/2}, F+1, m'_F\rangle$ , and  $n_x = n'_x, n_y = n'_y$ . The transition frequency  $\omega_R(\mathbf{n}, \mathbf{n}')$  is  $\omega_{12} + \Delta n_z \nu_z$ , where  $\omega_{12}$  is for the  $|\phi_1\rangle \rightarrow |\phi_2\rangle$  transition of a free atom and  $\Delta n_z = n'_z - n_z$ .

In practice, the Raman transition suffers an inhomogeneous broadening from anharmonicity of the potential well as well as from the usual differential ac Stark shift between  $|\phi_1\rangle$  and  $|\phi_2\rangle$ . For anharmonicity, we consider the quartic terms from  $U(\vec{r})$ :

$$W_q = U_0 \left( \frac{1}{3} k^4 z^4 + 2 \frac{k^2 \rho^2 z^2}{w_0^2} + 2 \frac{\rho^4}{w_0^4} \right), \quad (30)$$

where  $\rho^2 = x^2 + y^2$ . While the carrier frequency is not shifted by  $W_q$  in the first-order perturbation, the sidebands for  $\Delta n_z = \pm 1$  suffer a shift by  $\Delta\omega_q(\mathbf{n}, \mathbf{n}')$ :

$$\Delta\omega_q(\mathbf{n}, \mathbf{n}') = -\Delta n_z \left\{ \Delta\omega_q^{(1)} \left( n_z + \frac{1}{2} \right) + \Delta\omega_q^{(2)} (n_\perp + 1) \right\}, \quad (31)$$

where  $n_\perp = n_x + n_y$ ,  $\Delta\omega_q^{(1)} = \hbar k^2/2m$ , and  $\Delta\omega_q^{(2)} = k\hbar/\sqrt{2}mw_0$ . We neglect an offset term which is independent of  $\mathbf{n}$  and  $\mathbf{n}'$ . In addition, from the dependence of  $U_0$  on  $F$  and  $m_F$  in Eq. (10),  $\omega_R(\mathbf{n}, \mathbf{n}')$  is further shifted by  $\Delta\omega_\beta(\mathbf{n}, \mathbf{n}')$ :

$$\Delta\omega_\beta(\mathbf{n}, \mathbf{n}') = \Delta\omega_\beta^{(1)} \left( n_z + \frac{1}{2} \right) + \Delta\omega_\beta^{(2)} (n_\perp + 1), \quad (32)$$

where  $\Delta\omega_\beta^{(1)} = \{\eta\beta g_F(m_F + m'_F)/2\alpha\}\omega_z$  and  $\Delta\omega_\beta^{(2)} = \{\eta\beta g_F(m_F + m'_F)/2\alpha\}\omega_\perp$ . Here we assume  $|\Delta\alpha| \ll |\eta\beta g_F(m_F + m'_F)|$ , which is valid for a heavy alkali-metal atom in a circularly

polarized trap. From Eqs. (31) and (32), we note that the total shift  $\Delta\omega_q(\mathbf{n}, \mathbf{n}') + \Delta\omega_\beta(\mathbf{n}, \mathbf{n}')$  vanishes if  $\Delta\omega_\beta^{(1)} = \Delta n_z \Delta\omega_q^{(1)}$  and  $\Delta\omega_\beta^{(2)} = \Delta n_z \Delta\omega_q^{(2)}$ . Because the ratio  $\Delta\omega_q^{(1)}/\Delta\omega_q^{(2)}$  is the same as  $\Delta\omega_\beta^{(1)}/\Delta\omega_\beta^{(2)}$ , the two conditions are simultaneously satisfied when

$$|U_0| = \left[ \frac{\alpha}{\beta g_F(m_F + m'_F)} \right]^2 \frac{\hbar^2 k^2}{2m} \quad (33)$$

and  $\eta = \Delta n_z$ . We may call  $|U_0|$  a magic well depth. By using either a right or a left circularly polarized beam, the total shift can be eliminated for either blue or red sideband, respectively. If a trap beam is elliptically polarized with  $|\eta| < 1$ , the magic  $|U_0|$  increases by  $1/\eta^2$ , giving flexibility in designing an experiment.

We have experimentally demonstrated the idea of magic well depth by eliminating inhomogeneous broadening of a Raman sideband transition using  $^{87}\text{Rb}$  atoms trapped in a 1D optical lattice [7]. Figure 7 shows the lineshape of simulated Raman transitions: blue circles are for the transition of interest,  $|5S_{1/2}, F=1, m_F=-1\rangle \rightarrow |5S_{1/2}, F=2, m'_F=-1\rangle$ , and red squares are for the clock transition, whose broadening is only from the anharmonicity. We use a left circularly polarized lattice beam at  $\lambda_{\text{OL}} = 980$  nm and the magic well depth

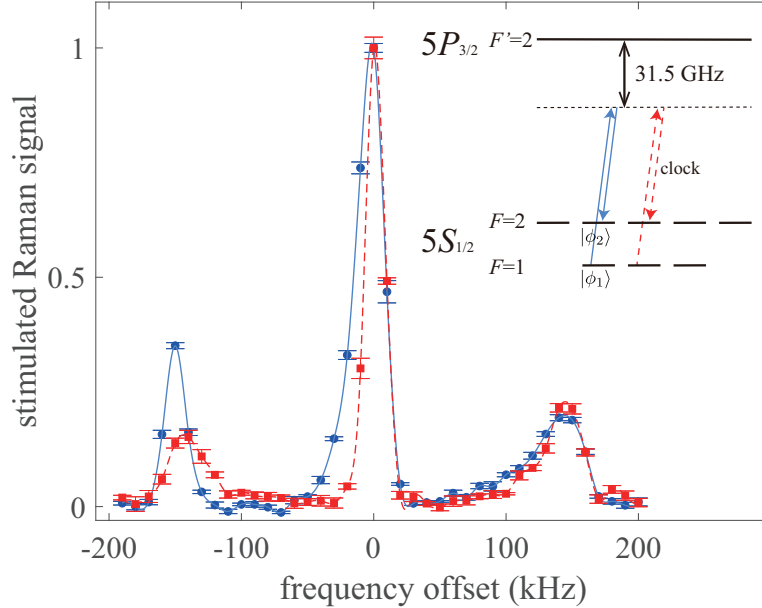


FIG. 7: Stimulated Raman spectrum at the magic well depth. Red sideband of the  $|5S_{1/2}, F=1, m_F=-1\rangle \rightarrow |5S_{1/2}, F=2, m'_F=-1\rangle$  transition (solid line with blue circles) is narrowed by cancellation of broadening from anharmonicity and vector polarizability. Spectrum of the clock transition (dashed line with red squares), which suffers broadening from only the anharmonicity, is shown for comparison. Each spectrum is normalized to its carrier signal.

of  $|U_0|/k_B = 140 \mu\text{K}$ , determined by  $\lambda_{\text{OL}}$  and the transition of interest. Focusing on the red sideband of both transitions, we observe the line-narrowing effect of magic well depth. The carrier of the clock transition is the narrowest because it is free from both  $\Delta\omega_q(\mathbf{n}, \mathbf{n}')$  and  $\Delta\omega_\beta(\mathbf{n}, \mathbf{n}')$ .

## VI. MOTION-SELECTIVE COHERENT POPULATION TRAPPING

RSC puts trapped atoms to the motional ground state with high probability only when the Lamb-Dicke parameter  $\eta_{\text{LD}} = \sqrt{\mathcal{E}_R/\hbar\nu}$  is much smaller than 1. Here,  $\mathcal{E}_R$  is the recoil energy accompanying the emission of a photon and  $\nu$  is the vibrational frequency of a trapped atom. While the condition is well satisfied along tightly confined directions in an optical lattice or an optical tweezer, it is difficult to satisfy the condition in a typical optical trap. To improve the effectiveness of RSC outside the Lamb-Dicke regime, we proposed to incorporate the phenomenon of coherent population trapping (CPT) to RSC [8]. Figure 8 shows the inverted Y configuration for the cooling scheme. A usual RSC (shown in black) consists of a red-detuned Raman transition  $|\phi_1\rangle \rightarrow |\phi_3\rangle$ , which we call  $p$  transition, and the  $D$  transition  $|\phi_3\rangle \rightarrow |\phi_4\rangle$  for optical pumping. To incorporate CPT, we add  $q$  Raman transition  $|\phi_2\rangle \rightarrow |\phi_3\rangle$  (shown in red) to form a  $\Lambda$  configuration. To make the CPT resonance condition dependent on the motional quantum number  $n$ , we use a circularly polarized trap beam so that  $\nu_1 \neq \nu_2$  owing to the vector polarizability. Here,  $\nu_1$  and  $\nu_2$  are the vibration frequencies of the motional states,  $|\chi_1\rangle$  and  $|\chi_2\rangle$ , for the potential wells of  $|\phi_1\rangle$  and  $|\phi_2\rangle$ , respectively. Their difference is

$$\Delta\nu_{12} = \frac{\beta}{4\alpha} \nu_0, \quad (34)$$

where  $\nu_0$  is the vibration frequency in a linearly polarized trap. When the  $p$  and  $q$  pairs of Raman beams are tuned to the  $\Lambda$  resonance between the  $|\phi_1, \chi_1(0)\rangle$  and  $|\phi_2, \chi_2(0)\rangle$  states, the motional ground states form a CPT dark state:

$$|\Psi(\text{CPT})\rangle = \frac{|\phi_1, \chi_1(0)\rangle - |\phi_2, \chi_2(0)\rangle}{\sqrt{2}}, \quad (35)$$

where atoms are accumulated. A pair of  $|\phi_1, \chi_1(n)\rangle$  and  $|\phi_2, \chi_2(n)\rangle$  states are detuned from the CPT resonance by  $n\Delta\nu_{12}$ , and a pair with the larger  $n$  is brighter. We call this method motion-selective coherent population trapping (MSCPT), and it is a trapped-atom analogue to the velocity-selective CPT developed for subrecoil cooling of free He atoms [31].



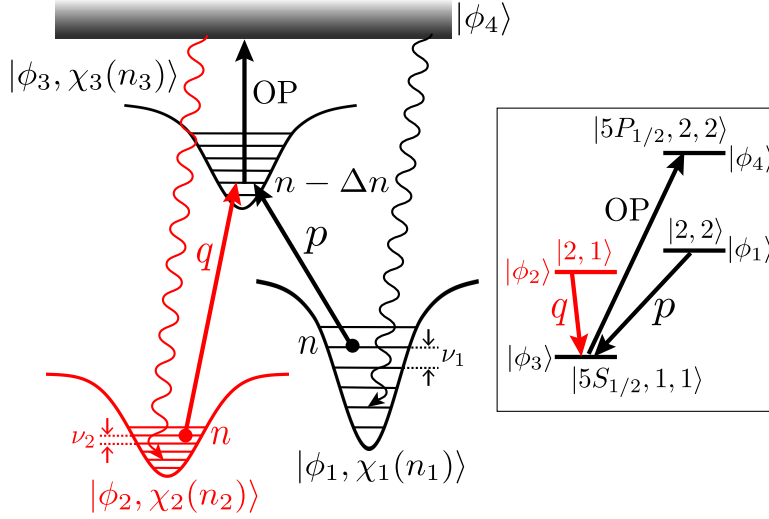


FIG. 8: Level schemes for RSC and inverted Y configuration of MSCPT experiment. RSC scheme is shown in black and  $q$  transition of MSCPT is shown in red. Specific levels and transitions in  $^{87}\text{Rb}$  are assigned in the inset.

Heavy alkali-metal atoms with large  $\beta$  are favored for MSCPT. For a  $^{87}\text{Rb}$  atom, if the trap wavelength is 850 nm and  $\eta_{LD} = 1$ ,  $\Delta\nu_{12}/2\pi = 75$  Hz, while FWHM of the CPT resonance in our radio frequency (rf) experiment was 150 Hz [32]. In the inset of Fig. 8, specific levels in  $^{87}\text{Rb}$  are assigned:  $|\phi_1\rangle = |5S_{1/2}, F = 2, m_F = 2\rangle$ ,  $|\phi_2\rangle = |2, 1\rangle$ ,  $|\phi_3\rangle = |1, 1\rangle$ , and  $|\phi_4\rangle = |5P_{1/2}, 2, 2\rangle$ . We note that the inverted Y configuration is closed owing to the angular momentum selection rule and, as a consequence, recoil heating during optical pumping is minimized.

Recently, we demonstrated the MSCPT cooling scheme in an experiment using  $^{87}\text{Rb}$  in a 1D optical lattice [9]. The lattice parameters were  $w_0 = 50$   $\mu\text{m}$ ,  $\lambda_{OL} = 980$  nm, and  $U_0/k_B = 125$   $\mu\text{K}$ , resulting in  $\eta_{LD} = 2.3$  and  $\Delta\nu_{12}/2\pi = 5$  Hz along the transverse direction. Although the parameters were not optimal for MSCPT because we used an apparatus originally built for a different experiment, we observed significant improvement in cooling efficiency compared with RSC when the detuning  $\delta_{\text{CPT}}(0)$  of the  $p$  and  $q$  Raman beams from the CPT resonance of the  $n = 0$  states was close to 0. In Fig. 9, temperature of the atoms in a steady state versus  $\delta_{\text{CPT}}(0)$  is shown for MSCPT (blue circles) and RSC (black triangles). To demonstrate the full benefit of the MSCPT scheme, we are upgrading the apparatus so that  $\eta_{LD} \simeq 1$  and  $\Delta\nu_{12} \geq 75$  Hz by using  $w_0 = 16$   $\mu\text{m}$ ,  $\lambda_{OL} = 850$  nm. Finally, we note that a diatomic polar molecule in an optical trap [33] provides an excellent

opportunity to apply MSCPT because its Stark shift depends strongly on the rotational quantum number. Considering a MgF molecule in a 532-nm optical trap as an example, the fractional difference between vibration frequencies of a pair of states in the same ro-vibrational level can be as large as 12%. This may be compared with  $\Delta\nu_{12}/\nu_0$  of less than 2% for  $^{87}\text{Rb}$  in the new design.

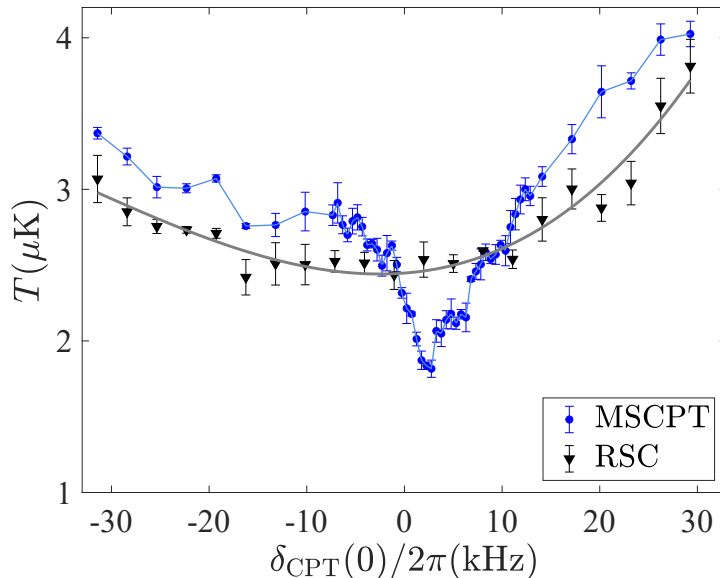


FIG. 9: Temperature versus detuning  $\delta_{\text{CPT}}(0)$  from the CPT resonance for the motional ground state. Blue circles represent results from MSCPT cooling scheme, and black triangles represent results when the  $p$  and  $q$  Raman beams are alternately turned on at 1 kHz.

## VII. CONCLUSION

Over the last two and a half decades, our laboratory at Korea University has proposed several ideas using vector polarizability to manipulate alkali-metal atoms and carried out experiments to demonstrate those ideas. In this paper, we reviewed the ideas and experimental results. Currently, we are working on an experiment to probe the cooling limit of a scheme based on motion-selective coherent population trapping and study strategies to apply the scheme to diatomic polar molecules in an optical trap.

## **ACKNOWLEDGMENTS**

This work was supported by the National Research Foundation of Korea (Grant No. NRF-2022R1F1A1075131).

## Appendix A: Numerical calculation of scalar and vector polarizabilities

In the Excel file of the Supplementary Material, to obtain numerical values of  $\alpha$  and  $\beta$ , we use the definitions in Eq. (8) and Eq. (9), respectively, including the off-resonant terms. Those terms are not negligible when a trap beam is far detuned. When the principal quantum number of the ground state of an alkali-metal atom is  $n$ , we include couplings to only the  $nP_{J'}$  and  $(n+1)P_{J'}$  states with  $J' = 1/2, 3/2$ . To obtain numerical values of  $a$  and  $b$ , we use Eq. (19) and Eq.(20), respectively, and restrict the sums to  $n' = n$ . Because we consider a far detuned trap beam, either ground or excited state hyperfine splitting is not important, and the effect of an isotope shift is negligible too.

There are two definitions for a reduced matrix element commonly used in the literature. We follow that of Racah [11], according to which the Wigner-Eckart theorem is written as [12]

$$\langle n', J', m'_J | d_q | n, J, m_J \rangle = (-1)^{J'-m'} \begin{pmatrix} J' & 1 & J \\ -m'_J & q & m_J \end{pmatrix} \langle n' J' || d || n J \rangle, \quad (\text{A1})$$

and the reduced matrix element for an electric dipole moment between the  $|n'P_{J'}\rangle$  and  $|nS_{1/2}\rangle$  states of an alkali-metal atom is related to the lifetime  $\tau(n'P_{J'})$  by

$$|\langle n'P_{J'} || d || nS_{1/2} \rangle|^2 = \frac{1}{\tau(n'P_{J'})} \frac{3\pi\epsilon_0\hbar c^3}{\omega_0^3} (2J' + 1), \quad (\text{A2})$$

where  $\omega_0$  is the  $|nS_{1/2}\rangle \rightarrow |n'P_{J'}\rangle$  transition frequency. For spectroscopic data, we use NIST Atomic Spectra Database Lines Data [13], where the Einstein coefficient  $A(n'P_{J'}) = 1/\tau(n'P_{J'})$  of the upper state  $|n'P_{J'}\rangle$  and the wavelength  $\lambda_0 = 2\pi c/\omega_0$  are tabulated.

In the Excel file, for a given wavelength  $\lambda$  of a trap beam,  $\alpha, \beta$  and  $a, b$  are calculated in atomic units. For a given power  $P$ , minimum spot size  $w_0$  ( $e^{-2}$  intensity radius), and degree of circularity  $\eta$  of the trap beam, the well depth  $U_{AC}(F, m_F)$  for the ground hyperfine state  $|nS_{1/2}, F, m_F\rangle$  according to Eq. (10) is given (in mK) by

$$U_{AC}(F, m_F) = (\alpha - \eta\beta g_F m_F)(c\mu_0 I_0/2). \quad (\text{A3})$$

The photon scattering rate  $R_\gamma(F, m_F)$  according to Eq. (18) is given (in  $\text{s}^{-1}$ ) by

$$R_\gamma(F, m_F) = (a - \eta b g_F m_F)(c\mu_0 I_0/2)\Gamma, \quad (\text{A4})$$

where we use  $\Gamma = A(nP_{1/2})$  of the  $D_1$  transition.

- 
- [1] D. Cho, Analogous Zeeman Effect from the Tensor Polarizability in Alkali Atoms, J. Korean Phys. Soc. **30**, 373 (1997).
  - [2] C. Y. Park, H. Noh, C. M. Lee, and D. Cho, Measurement of the Zeeman-like ac Stark shift Phys. Rev. A **63**, 032512 (2001). DOI: 10.1103/PhysRevA.63.032512
  - [3] C. Y. Park, J. Y. Kim, J. M. Song, and D. Cho, Optical Stern-Gerlach effect from the Zeeman-like ac Stark shift, Phys. Rev. A **65**, 033410 (2002). DOI: 10.1103/PhysRevA.65.033410
  - [4] K. L. Corwin, S. J. M. Kuppens, D. Cho, and C. E. Wieman, Spin-Polarized Atoms in a Circularly Polarized Optical Dipole Trap, Phys. Rev. Lett. **83**, 1311 (1999). DOI: 10.1103/PhysRevLett.83.1311
  - [5] J. M. Choi and D. Cho, Elimination of inhomogeneous broadening for a ground-state hyperfine transition in an optical trap, J. Phys. Conf. Ser. **80**, 012037 (2007). doi:10.1088/1742-6596/80/1/012037
  - [6] H. Kim, H. S. Han, and D. Cho, Magic Polarization for Optical Trapping of Atoms without Stark-Induced Dephasing, Phys. Rev. Lett. **111**, 243004, (2013). DOI: 10.1103/PhysRevLett.111.243004
  - [7] M. H. Seo, S. Park, and D. Cho, Relaxation of atomic temperature anisotropy in a one-dimensional optical lattice enhanced by dynamic control of the aspect ratio, Phys. Rev. A **101**, 043611 (2020). DOI: 10.1103/PhysRevA.101.043611
  - [8] H. G. Lee, S. Park, M. H. Seo, and D. Cho, Motion-selective coherent population trapping for subrecoil cooling of optically trapped atoms outside the Lamb-Dicke regime, Phys. Rev. A **106**, 023324 (2022). DOI: 10.1103/PhysRevA.106.023324
  - [9] S. Park, M. H. Seo, R. A. Kim, and D. Cho, Motion-selective coherent population trapping by Raman sideband cooling along two paths in a  $\Lambda$  configuration, Phys. Rev. A **106**, 023323 (2022). DOI: 10.1103/PhysRevA.106.023323
  - [10] A. Khadjavi, A. Lurio, and W. Happer, Stark Effect in the Excited States of Rb, Cs, Cd, and Hg\*, Phys. Rev. **167**, 128 (1968). DOI: 10.1103/PhysRev.167.128
  - [11] G. Racah, Theory of complex spectra. II, Phys. Rev. **62**, 438, (1942). DOI: 10.1103/PhysRev.62.438
  - [12] A. R. Edmonds, *Angular Momentum in Quantum Mechanics* (Princeton University Press,

- Princeton, New Jersey, 1960), p.75.
- [13] <http://physics.nist.gov/cgi-bin/ASD/energy1.pl>
  - [14] Z. T. Lu, K. L. Corwin, M. J. Renn, M. H. Anderson, E. A. Cornell, and C. E. Wieman, Low-Velocity Intense Source of Atoms from a Magneto-optical Trap, *Phys. Rev. Lett.* **77**, 3331 (1996). DOI: 10.1103/PhysRevLett.77.3331
  - [15] R. J. Cook, Optical Stern-Gerlach effect, *Phys. Rev. A* **35**, 3844 (1987). DOI: 10.1103/PhysRevA.35.3844
  - [16] T. Sleator, T. Pfau, V. Balykin, O. Carnal, and J. Mlynek, Experimental Demonstration of the Optical Stern-Gerlach effect, *Phys. Rev. Lett.* **68**, 1996 (1992). DOI: 10.1103/PhysRevLett.68.1996
  - [17] M. Karski, L. Förster, J. M. Choi, A. Steffen, W. Alt, D. Meschede, and A. Widera, Quantum Walk in Position Space with Single Optically Trapped Atoms, *Science* **325**, 174 (2009). DOI: 10.1126/science.1174436
  - [18] M. Anderlini, P. J. Lee, B. L. Brown, J. Sebby-Strabley, W. D. Phillips, and J. V. Porto, Controlled exchange interaction between pairs of neutral atoms in an optical lattice, *Nature* **448**, 452 (2007). doi:10.1038/nature06011
  - [19] J. Y. Kim, J. S. Lee, J. H. Han, and D. Cho, Optical Dipole Trap without Inhomogeneous ac Stark Broadening, *J. Korean Phys. Soc.* **42**, 483 (2003).
  - [20] S. Kuhr, W. Alt, D. Schrader, I. Dotsenko, Y. Miroshnychenko, A. Rauschenbeutel, and D. Meschede, Analysis of dephasing mechanisms in a standing-wave dipole trap, *Phys. Rev. A* **72**, 023406 (2005). DOI: 10.1103/PhysRevA.72.023406
  - [21] A. Kaplan, M. F. Andersen, and N. Davidson, Suppression of inhomogeneous broadening in rf spectroscopy of optically trapped atoms, *Phys. Rev. A* **66**, 045401 (2002). DOI: 10.1103/PhysRevA.66.045401
  - [22] A. G. Radnaev, Y. O. Dudin, R. Zhao, H. H. Jen, S. D. Jenkins, A. Kuzmich and T. A. B. Kennedy, A quantum memory with telecom-wavelength conversion, *Nat. Phys.* **6**, 894 (2010). DOI: 10.1038/NPHYS1773
  - [23] Y. Sagi, I. Almog, and N. Davidson, Process Tomography of Dynamical Decoupling in a Dense Cold Atomic Ensemble, *Phys. Rev. Lett.* **105**, 053201 (2010). DOI: 10.1103/PhysRevLett.105.053201
  - [24] N. Davidson, H. J. Lee, C. S. Adams, M. Kasevich, and S. Chu, Long Atomic Coherence

- Times in an Optical Dipole Trap, *Phys. Rev. Lett.* **74**, 1311 (1995). DOI: 10.1103/PhysRevLett.74.1311
- [25] V. V. Flambaum, V. A. Dzuba, and A. Derevianko, Magic Frequencies for Cesium Primary-Frequency Standard, *Phys. Rev. Lett.* **101**, 220801 (2008). DOI: 10.1103/PhysRevLett.101.220801
- [26] M. S. Safronova, U. I. Safronova, and C. W. Clark, Magic wavelengths for optical cooling and trapping of lithium, *Phys. Rev. A* **86**, 042505 (2012). DOI: 10.1103/PhysRevA.86.042505
- [27] H. S. Han, H. G. Lee, and D. Cho, Site-Specific and Coherent Manipulation of Individual Qubits in a 1D Optical Lattice with a 532-nm Site Separation, *Phys. Rev. Lett.* **122**, 133201 (2019). DOI: 10.1103/PhysRevLett.122.133201
- [28] K. Kwon, K. Kim, J. Hur, S. Huh, and J. Choi, Site-resolved imaging of a bosonic Mott insulator of  $^7\text{Li}$  atoms, *Phys. Rev. A* **105**, 033323 (2022). DOI: 10.1103/PhysRevA.105.033323
- [29] A. Derevianko, Theory of magic optical traps for Zeeman-insensitive clock transitions in alkali-metal atoms, *Phys. Rev. A* **81**, 051606(R) (2010). DOI: 10.1103/PhysRevA.81.051606
- [30] C. Monroe, D. M. Meekhof, B. E. King, S. R. Jefferts, W. M. Itano, D. J. Wineland, and P. Gould, Resolved-Sideband Raman Cooling of a Bound Atom to the 3D Zero-Point Energy, *Phys. Rev. Lett.* **75**, 4011 (1995). DOI: 10.1103/PhysRevLett.75.4011
- [31] A. Aspect, E. Arimondo, R. Kaiser, N. Vansteenkiste, and C. Cohen-Tannoudji, Laser Cooling below the One-Photon Recoil Energy by Velocity-Selective Coherent Population Trapping, *Phys. Rev. Lett.* **61**, 826 (1988). DOI: 10.1103/PhysRevLett.61.826
- [32] H. Kim, H. S. Han, T. H. Yoon, and D. Cho, Coherent Population Trapping in a  $\Lambda$  Configuration Coupled by Magnetic Dipole Interactions, *Phys. Rev. A* **89**, 032507 (2014). DOI: 10.1103/PhysRevA.89.032507
- [33] L. Anderegg, B. L. Augenbraun, Y. Bao, S. Burchesky, L. W. Cheuk, W. Ketterle, and J. M. Doyle, Laser Cooling of Optically Trapped Molecules, *Nat. Phys.* **14** 890 (2018). DOI: 10.1038/s41567-018-0191-z